Conference materials
UDC 538.958
DOI: https://doi.org/10.18721/JPM.161.216

Thermal characteristics of III-V microlasers bonded onto silicon board

A.S. Dragunova [1]✉, N.V. Kryzhanovskaya [1,2], F. I. Zubov [1,2], E. I. Moiseev [1], A.M. Nadtochiy [1,3], N.A. Fominykh [1], K.A. Ivanov [1], M.V. Maximov [1,2], A.A. Vorobyev [2], A.M. Mozharov [2], N.A. Kalyuzhnyy [3], S.A. Mintairov [3], N.Yu. Gordeev [3], Yu.A. Guseva [3], M.M. Kulagina [3], A.E. Zhukov [1]

[1] HSE University, St. Petersburg, Russia;
[2] Alferov University, St. Petersburg, Russia;
[3] Ioffe Institute, St Petersburg, Russia
✉ anndra@list.ru

Abstract. In this work, we study the characteristics of semiconductor microlasers based on the heterostructure with two coupled waveguides intended to improve heat dissipation in cw regime. We analysed total output optical loss of the microlasers, their spectral characteristics, output power, emission pattern and thermal resistance. We observed that the use of the principle of two coupled resonant planar waveguides, active and passive, as well as p-side down bonding, significantly reduces the thermal resistance of microlasers and improves their performance.

Keywords: hybrid integration, microlaser, quantum well dots, thermal resistance

Funding: This study was supported by Russian Science Foundation grant 18-12-00287, https://rscf.ru/project/18-12-00287/. Support of optical measurements was implemented in the framework of the Basic Research Program at the National Research University Higher School of Economics (HSE University).

Citation: Dragunova A.S., Kryzhanovskaya N.V., Zubov F.I., Moiseev E. I., Nadtochiy A.M., Fominykh N.A., Ivanov K. A., Maximov M.V., Vorobyev A.A., Mozharov A. M., Kalyuzhnyy N. A., Gordeev N. Yu, Guseva Yu. A., Kulagina M. M., Zhukov A.E., Thermal characteristics of III-V microlasers bonded onto silicon board, St. Petersburg State Polytechnical University Journal. Physics and Mathematics. 16 (1.2) (2023) 108–113. DOI: https://doi.org/10.18721/JPM.161.216

Материалы конференции
УДК 538.958
DOI: https://doi.org/10.18721/JPM.161.216

Тепловые характеристики микролазеров III-V, перенесенных на кремниевую подложку

А.С. Драгунова [1]✉, Н.В. Крыжановская [1,2], Ф.И. Зубов [1,2], Э.И. Моисеев [1], А.М. Надточий [1,3], Н.А. Фоминых [1], К.И. Иванов [1], М.В. Максимов [1,2], А.А. Воробьев [2], А.М. Можаров [2], Н.А. Калюжный [3], С.А. Минтаиров [3], Н.Ю. Гордеев [3], Ю.А. Гусева [3], М.М. Кулагина [3], А.Е. Жуков [1]

[1] Национальный исследовательский университет «Высшая школа экономики», Санкт-Петербург, Россия;
[2] Академический университет им. Ж.И. Алфёрова, Санкт-Петербург, Россия;
[3] Физико-технический институт им. А.Ф. Иоффе РАН, Санкт-Петербург, Россия;
✉ anndra@list.ru

Аннотация. В данной работе исследуются характеристики полупроводниковых микролазеров на основе гетероструктуры с двумя связанными волноводами, предназначенных для улучшения теплоотвода в непрерывном режиме. Были проанализированы полные выходные оптические потери микролазеров, их спектральные характеристики, выходная мощность, диаграмма направленности излучения и тепловое сопротивление. Отметим, что использование принципа двух связанных резонансных планарных волноводов, активного и пассивного, а также соединения p-стороной вниз значительно снижает тепловое сопротивление микролазеров и улучшает их характеристики.

Ключевые слова: гибридная интеграция, микролазер, квантовые яма-точки, тепловое сопротивление

Финансирование: Исследование выполнено при поддержке гранта РНФ18-12-00287, https://rscf.ru/project/18-12-00287/. Оптические измерения осуществлены в рамках Программы фундаментальных исследований НИУ ВШЭ.

Ссылка при цитировании: Драгунова А.С., Крыжановская Н.В., Зубов Ф.И., Моисеев Э.И., Надточий А.М., Фоминых Н.А., Иванов К.А., Максимов М.В., Воробьев А.А., Можаров А.М., Калюжный Н.А., Гордеев Н.Ю., Гусева Ю.А., Кулагина М.М., Жуков А.Е. Исследование тепловых характеристик микролазеров III-V, перенесенных на кремниевую подложку // Научно-технические ведомости СПбГПУ. Физико-математические науки. 2023. Т. 16. № 1.2. С. 108–113. DOI: https://doi.org/10.18721/JPM.161.216

Introduction

The self-heating effects of cw-operating diode lasers, associated with the incomplete conversion of the supplied electric power into light power, are especially critical for devices with a small surface area, such as microdisk lasers [1]. The active region is the main source of Joule heat in a semiconductor lasers. Depending on the bonding side, heat can be removed mainly in two directions: towards the relatively thin upper epitaxial layers and towards the substrate. One option to reduce thermal resistance is to optimize the design of the laser structure. The standard total thickness of the upper contact layer, the upper p-cladding layer and the upper part of waveguide layer is about 2–2.5 μm. The upper p-cladding layer makes the largest contribution to this thickness (about 1.5 μm). It must effectively confine the fundamental optical mode within the vertical waveguide. As the cladding layer thickness decreases, the mode begins to penetrate into the highly doped upper contact layer, that leads to a catastrophic increase in internal optical losses up to the disruption of lasing. The solution to the problem is to use the principle of two coupled resonant planar waveguides, of which one is active and another is passive [2]. An active waveguide contains an active region and fundamental mode. High-order modes resonantly tunnels into an optically coupled passive waveguide. Also, to reduce further the thermal resistance and ensure maximum heat dissipation, one can mount lasers on a metal or ceramic heat sink with epitaxial layers down (p-side down).

In this work, we study the characteristics of microlasers developed from the heterostructure with two coupled resonant planar waveguides, active and passive. The effect of thermal resistance reduction on the output power before and after bonding was investigated.

Materials and Methods

Growth of the laser structure was carried out using metalorganic vapour-phase epitaxy on n+-GaAs substrate misoriented by 6o towards [111] direction. The laser structure consisted of an $Al_{0.25}Ga_{0.75}As$ n-cladding layer with a thickness of 1.2 μm, a passive n-GaAs waveguide with a thickness of 0.55 μm, an n-$Al_{0.25}Ga_{0.75}As$ optical barrier, a main undoped GaAs waveguide with a thickness of 1.37 μm, an upper p-$Al_{0.25}Ga_{0.75}As$ cladding layer of 0.5 μm and upper p-GaAs contact

layer 0.15 μm thick (Fig. 1). The active region consisted of 5 layers of InGaAs quantum well dots. Within the waveguide layer, the active region was shifted towards the upper cladding layer and was located at a distance of 220 nm from it. Its location was chosen to be in the minimum of the second-order vertical mode. Lasing via the first-order mode (green line in Fig. 1) is suppressed due to its resonant leakage into the optically coupled passive waveguide. Thus, we managed to locate the active region at a distance of only 870 nm from the top surface of the heterostructure.

To support the effect of optical tunneling between the two waveguides it is necessary that the effective refractive indices of the interacting modes coincide, and the distance between the waveguides be comparable to the depth of mode penetration into the waveguide cladding. The effective refractive index of the mode increases with the thickness of the waveguide and/or the contrast of the refractive index between the materials of the waveguide layer and the cladding. Therefore, it is possible to design waveguides in such a way that one of the high-order modes of the wide, main waveguide will coincide in effective refractive index with the fundamental mode of the narrow, additional waveguide. If the active medium is located in a multimode (active) waveguide, then a high-order mode resonantly tunnels into a single-mode waveguide and is excluded from laser generation due to a decrease in the optical confinement factor, as well as additional losses in the passive waveguide. The fundamental mode of the multimode waveguide does not change in this case. The advantage of this approach is the possibility of expanding the waveguide thickness in the vertical direction and selective suppression of high-order modes, as well as a decrease in the thickness of the p-emitter layer.

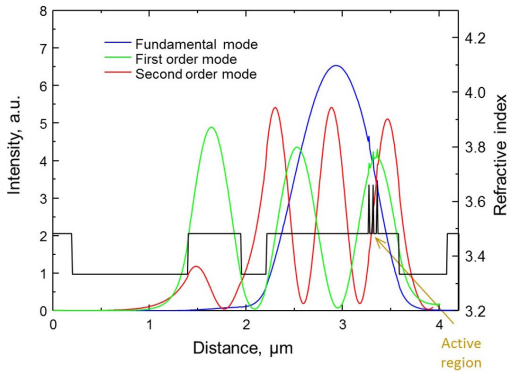

Fig. 1. Structure's refractive index profile and transverse optical modes intensity profiles

Laser mesas were formed with a diameter of 30–50 μm using plasma etching through the active region to the buffer layer. Metal contacts were formed using AuGe/Ni/Au and AgMn/Ni/Au for n- and p-contacts, respectively. Four different types of laser mesas with contacts were formed: microdisk lasers (D), microring lasers with 50 and 30 μm outer diameter and 30 μm (assigned as RB) and 18 μm (assigned as RS) inner diameter. The Au-Au thermocompression bonding of microdisk lasers to the silicon surface was performed using a Finetech FINEPLACERlambda2 setup. Electroluminescence spectra were recorded using a 20x objective, Horiba FHR 1000 monochromator and InGaAs CCD (spectral resolution 30 pm) or, for measurements over a wide spectral range, a Yokogawa AQ6370C optical spectrum analyser was used. The far field emission pattern was obtained using a setup for measuring the spectral-angular dependences of the lasing intensity.

Results and Discussion

First, broad-area (BA) lasers with a stripe width of 100 μm and a stripe length (L) of 200–4000 μm were formed from the grown epitaxial structure. BA lasers operating in the CW-mode at room temperature have a lasing wavelength that strongly depends on the stripe length (Fig. 2, *a*). Such a change in wavelength is associated with losses in the laser. We have studied the dependence of the differential quantum efficiency on the length of the resonator, and we determined the internal optical losses α_{in}, which amounted to only 0.7 cm^{-1} and a high internal quantum efficiency of stimulated emission $\eta_{in} = 79\%$. According to the formula $\alpha_{in} + (1/L) \ln(1/R)$, where $R = 0.3$ is the facet reflectivity, we calculated the dependences of the total optical losses in a laser depending on

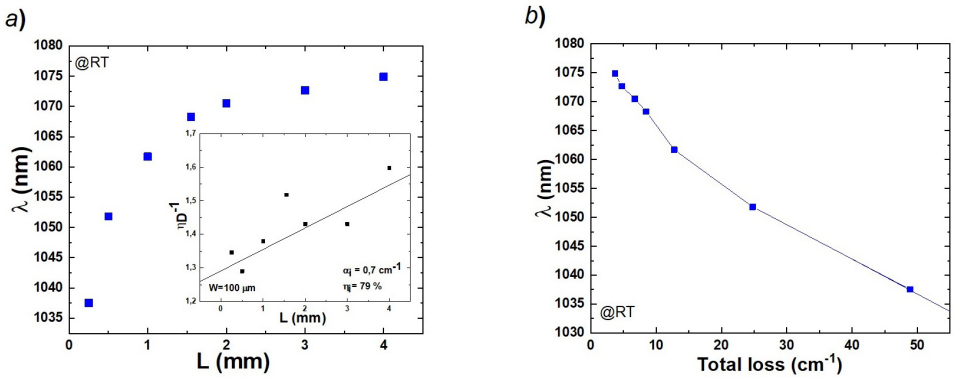

Fig. 2. Dependence of the lasing wavelength on the stripe length, inset: dependence of the external differential efficiency on the stripe length (*a*), dependence of the total optical losses on the lasing wavelength for BA lasers (*b*)

the lasing wavelength (Fig. 2, *b*). From the experimental dependence of the lasing wavelength on the total loss we can estimate the total optical loss for microlasers using their emission wavelength.

We have studied, lasing spectra of the microlasers at room temperature without bonding. Example of the lasing spectra obtained for microdisk lasers are presented in Fig. 3. With decreasing of the microdisk laser diameter we observe the tendency toward a decrease in the lasing wavelength and an increase in the threshold current density (Fig. 4), which is explained by an increase in losses in the microdisk laser. In accordance with the data of Fig. 2, *b* and 3, the total optical loss for a microdisk laser increases from 13.6 cm^{-1} for a diameter of 50 μm to 58 cm^{-1} for a diameter of 30 μm.

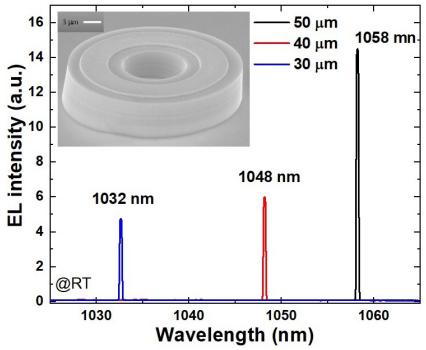

Fig. 3. Electroluminescence spectra for microdisk lasers with a diameter of 30, 40, and 50 μm

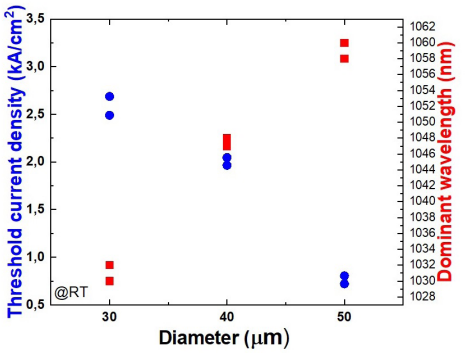

Fig. 4. Lasing wavelength and threshold current vs microdisk diameter (data was obtained for two microlasers of each diameter)

Next we compared the thermal resistance for different types of microlasers with a diameter of 30 and 50 μm before and after bonding to a Si substrate (Fig. 5). For microlasers with a diameter of 30 μm, the thermal resistance was observed at a level of 0.55 K/mW for all types of microlasers before bonding. The value of the thermal resistance for a single-waveguide microdisk laser with a diameter of 30 μm was obtained in [3] to be 0.59 K/mW, which is slightly larger than the value obtained for our microdisk laser with the same diameter. After bonding a decrease in thermal resistance by a factor of about 2–3 is observed for all the microlasers. In our microdisk lasers, the value of thermal resistance after bonding decreased to 0.22 K/mW, while for a single-waveguide microdisk laser, this value decreased to 0.32 K/mW. Based on this comparison, we can conclude that the use of the principle of two coupled resonant active and passive planar waveguides makes it possible to reduce the thermal resistance of microlasers.

We also studied the dependence of thermal resistance on the microlaser type for lasers with a diameter of 50 μm before bonding. Fig. 5, *b* shows that, the thermal resistance of the microlaser increases with a decrease of its area. After bonding, regardless of the type of microlaser, the thermal resistance decreases to ~ 0.15 K/mW.

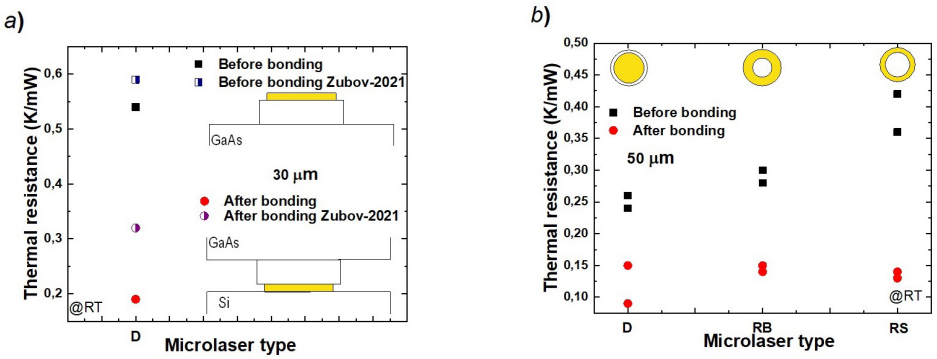

Fig. 5. Thermal resistance before and after bonding against microlaser type for 30 μm (*a*) and 50 μm (*b*)

Reducing thermal resistance improves various characteristics of microlasers. Increase of the output power after bonding was observed for all the devices studied. An example of a change in the output optical power is shown in Figure 6. Also, a decrease in thermal resistance after bonding led to an increase in the output power with the slope of power dependence and increase of the bias current of the thermal roll-over.

Next the far-field emission pattern was obtained for a microdisk laser with a diameter of 50 μm at various injection currents (Fig. 7). To study the far-field emission pattern, a different detector was used than the detector for collecting the output optical power, thus only a fraction of the output signal in a small azimuth angle was collected. We observe an interference pattern with the maximum emission power concentrated in the first two fringes with polar angles of 2° and 8°. This pattern is due to the interference of the direct and reflected from the planar etched GaAs surface output light of the microlaser. The angular position of the fringes depends only on the active region height above the bottom GaAs surface [4]. By fitting this dependence with a model that represents the output as a Gaussian beam, we can estimate the waist radius to be $r_0 \approx 0.9$ μm and thus the aperture (beam divergence) calculated with a well-known formula is $2\alpha = 2\lambda/(\pi r_0) \approx 40°$.

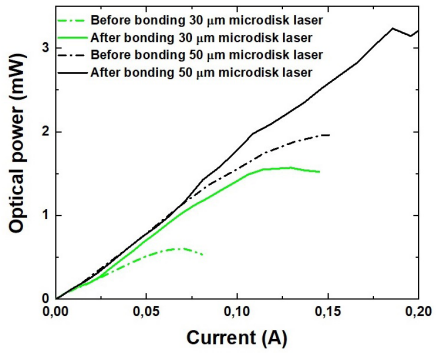

Fig. 6. The dependence of the output optical power on a threshold

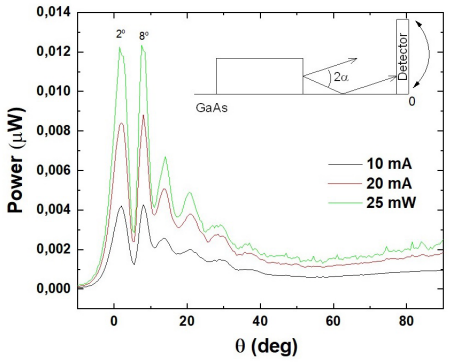

Fig. 7. The vertical far-field emission pattern for 50 μm microdisk laser

Conclusion

The total optical loss for microlasers with different diameters was calculated. The intensity peak positions on the emission pattern of 50 μm microlaser stayed unchanged with the increase of the injection current. The use of the principle of two coupled resonant planar waveguides active and passive, as well as p-side down bonding, can significantly reduce the thermal resistance of microlasers. A decrease in thermal resistance leads to an improvement in the characteristics of microlasers, including an improvement in the maximum optical power.

Acknowledgments

This study was supported by Russian Science Foundation grant 18-12-00287, https://rscf.ru/project/18-12-00287/. Support of optical measurements was implemented in the framework of

the Basic Research Program at the National Research University Higher School of Economics (HSE University).

REFERENCES

1. **Zhukov A.E., et al.,** Impact of self-heating and elevated temperature on performance of quantum dot microdisk lasers, IEEE Journal of Quantum Electronics. 56 (5) (2020) 1–8.

2. **Gordeev N.Y., et al.,** Transverse single-mode edge-emitting lasers based on coupled waveguides, Optics Letters. 40 (9) (2015) 2150–2152.

3. **Zubov F., et al.,** Improved performance of InGaAs/GaAs microdisk lasers epi-side down bonded onto a silicon board,Optics Letters. 46 (16) (2021) 3853–3856.

4. **Kadinskaya S.A., et al.,** Experimental investigation of the far-field emission pattern of microdisk laser modes, Journal of Physics: Conference Series. – IOP Publishing, 1695 (1) (2020) 012094.

THE AUTHORS

DRAGUNOVA Anna S.
anndra@list.ru
ORCID: 0000-0002-0181-0262

KRYZHANOVSKAYA Natalia V.
nataliakryzh@gmail.com
ORCID: 0000-0002-4945-9803

ZUBOV Fedor I.
fedyazu@mail.ru
ORCID: 0000-0002-3926-8675

MOISEEV Eduard I.
emoiseev@hse.ru
ORCID: 0000-0003-3686-935X

NADTOCHIY Alexey M.
al.nadtochy@mail.ioffe.ru
ORCID: 0000-0003-0982-907X

FOMINYKH Nikita A.
fominy-nikita@yandex.ru
ORCID: 0000-0003-3919-6410

IVANOV Konstantin I.
kivanov1992@gmail.com
ORCID: 0000-0003-2165-1067

MAXIMOV Mikhail V.
maximov.mikh@gmail.com
ORCID: 0000-0002-9251-226X

VOROBYEV Alexandr A.
alex.spbpu@mail.ru
ORCID: 0000-0003-2077-1243

MOZHAROV Alexey M.
alex000090@gmail.com
ORCID: 0000-0002-8661-4083

KALYUZHNYY Nikolay A.
Nickk@mail.ioffe.ru
ORCID: 0000-0001-8443-4663

MINTAIROV Sergey A.
mintairov@scell.ioffe.ru
ORCID: 0000-0002-6176-6291

GORDEEV Nikita Yu.
Gordeev@switch.ioffe.ru
ORCID: 0000-0002-9919-4794

GUSEVA Yulia A.
Guseva.Julia@mail.ioffe.ru
ORCID: 0000-0002-7035-482X

KULAGINA Marina M.
Marina.Kulagina@mail.ioffe.ru
ORCID: 0000-0002-8721-185X

ZHUKOV Alexey E.
zhukale@gmail.com
ORCID: 0000-0002-4579-0718

Received 29.09.2022. Approved after reviewing 09.11.2022. Accepted 11.11.2022.